Recognition of peptidoglycan and β-lactam antibiotics by the extracellular domain of the Ser/Thr protein kinase StkP from *Streptococcus pneumoniae*

Beatriz Maestro[1†], Linda Nováková[2], Dusan Hesek[3], Mijoon Lee[3], Eduardo Leyva[1], Shahriar Mobashery[3], Jesús M. Sanz[1]* and Pavel Branny[2]

[1] Instituto de Biología Molecular y Celular, Universidad Miguel Hernández, Elche, Spain
[2] Institute of Microbiology, v.v.i., Academy of Sciences of the Czech Republic, Prague, Czech Republic
[3] Department of Chemistry and Biochemistry, University of Notre Dame, Notre Dame, IN 46556, USA
† Present address: Instituto Universitario de Electroquímica. Universidad de Alicante. San Vicente del Raspeig. 03080- Alicante, Spain.

ABSTRACT. The eukaryotic-type serine/threonine kinase StkP from *Streptococcus pneumoniae* is an important signal-transduction element that regulates the expression of numerous pneumococcal genes. We have expressed the extracellular domain of this protein (C-StkP), elaborated a three-dimensional structural model and performed a spectroscopical characterization of its structure and stability. Biophysical experiments show that C-StkP binds to synthetic samples of the cell wall peptidoglycan and to β-lactam antibiotics, which mimic the terminal portions of the peptidoglycan stem peptide. This is the first experimental report on the recognition of a minimal peptidoglycan unit by a PASTA-containing kinase, suggesting that non-crosslinked peptidoglycan may act as a signal for StkP function and pointing to this protein as an interesting target for β-lactam antibiotics.

Keywords: *Streptococcus pneumoniae*, Signal transduction, PASTA domains, Peptidoglycan, β-lactam antibiotics, Protein structure

Abbreviations: PASTA domain, penicillin-binding protein and Ser/Thr protein kinase-associated domain; STPK, eukaryotic-type Ser/Thr protein kinase; C-StkP, C-terminal domain of StkP kinase; CD, circular dichroism; PGN, peptidoglycan; 6-APA, 6-aminopenicillanic acid; NAG, N-acetylglucosamine.

* To whom correspondence should be addressed: Instituto de Biología Molecular y Celular, Edificio Torregaitán, Universidad Miguel Hernández, 03202-Elche, Spain. Phone: +34 966658460; Fax: +34 966658758; E-mail: jmsanz@umh.es

INTRODUCTION

One of the most prevalent prokaryotic signal-transduction mechanisms involves the participation of histidine kinases that promote transcription of target genes by phosphorylation of their cognate response regulators [1,2]. However, recent studies have suggested that the eukaryotic-type Ser/Thr protein kinases (STPKs), which are abundantly present in prokaryotes [3,4], may constitute an independent signaling network. In contrast to the case of their eukaryotic counterparts, the signals to which prokaryotes respond, the mechanisms of signal transduction, and their substrates, remain poorly understood.

Certain Gram-positive bacterial STPKs are transmembrane proteins. These proteins are predicted to comprise an N-terminal intracellular kinase domain and a C-terminal extracellular domain, linked by a transmembrane segment [5]. The extracellular element contains several repeats of approximately 70 amino acids with the so-called PASTA signature sequence (for "Penicillin-binding protein And Ser/Thr protein kinase Associated") [6]. The three-dimensional structure of the two consecutive PASTA sequences of penicillin-binding protein PBP2x from *Streptococcus pneumoniae* [7] and the four-modular extracellular domain of PknB from *Mycobacterium tuberculosis* [8] are the only ones reported to date. In every case, each PASTA domain consists of a globular fold formed by an α-helix packed onto a three-stranded antiparallel β-sheet, but their spatial arrangement in PknB is much more extended than in PBP2x, where a strong interaction between domains occur. Moreover, the elucidation of the crystal structure of PBP2x in the presence of cefuroxime, a β-lactam antibiotic [9], indicated the binding of this molecule to one PASTA motif through loose interactions. Since the structures of ß-lactam antibiotics mimic the terminal portion of the peptidoglycan stem peptide [10], it was hypothesized that this domain is likely to bind the non-crosslinked peptidoglycan as well [6].

Therefore, STPKs containing PASTA modules could act as sensors for the presence of non-crosslinked peptidoglycan and transmit environmental cues into the cell accordingly. In this vein, Shah *et al.* [11] have recently shown that crude preparation of muropeptides are indeed effector molecules that interact with PrkC, a transmembrane STPK from *Bacillus subtilis*, resulting in activation of PrkC-dependent phosphorylation pathway and subsequent germination of dormant *B. subtilis* spores. A similar activation mechanism has also been suggested for *Mycobacterium tuberculosis* PknB [8], although no experimental evidence has been provided so far.

In previous studies we have characterized the eukaryotic-type Ser/Thr protein kinase StkP from *S. pneumoniae*. Biochemical [12] and microarray [13] analyses revealed that StkP dimerizes and controls expression of a wide set of genes encoding functions involved in important cellular processes. Moreover, the C-terminal domain of StkP is predicted to include four consecutive PASTA motifs [14]. In an attempt to investigate possible activators for StkP signaling, we report here biophysical studies that aim to demonstrate that both β-lactam antibiotics and small synthetic samples of peptidoglycan bind to the PASTA motifs of C-StkP, and therefore, may regulate the complex signal network controlled by the full-length kinase.

MATERIALS AND METHODS

Materials. StkP ligands (Fig. 1) were obtained as follows: Ampicillin (compound **1**) was purchased from Sigma-Aldrich, and 6-aminopenicillanic acid (6-APA) (compound **2**) was acquired from Fluka. The D-Ala-D-Ala dipeptide was from Bachem. The synthetic samples of the cell wall fragments **3** and **4** were synthesized as previously described [15,16].

Homology modeling. The PHYRE server (http://www.sbg.bio.ic.ac.uk/~phyre/) allowed the identification of cefuroxime-bound PBP2x (PDB code 1QMF) [9] as a suitable template for C-StkP homology modeling. Since the template only contains 2 PASTA domains, we first modeled each of the four PASTA sequences of C-StkP individually, and then linked them together using the SwissPDB utilities [17]. Loops connecting the PASTA domains were assigned random-coil conformations according to the secondary structure prediction by PHYRE. Structures were subjected to steepest descent energy minimization. Figures were rendered using the software package PyMol (Delano Scientific LLC).

Molecular biology procedures. In order to construct the pC-Stk1 plasmid to allow the overexpression and purification of histidine-tagged C-terminal domain of StkP (C-StkP protein), a DNA fragment comprising amino acid residues 363 to 659 of the full-length StkP was amplified by PCR using the oligonucleotides LN54 (5'-CGGCCATATGTCCAGATCTCCTGCAACCA-3') and StkP-R (5'-TTGATTATGAATTCGCTTTTAAGGAGTAGC-3') and plasmid pEXStkP [14] as template. The PCR fragment was digested with the *Nde*I and *Eco*RI restriction enzymes and ligated into the pET-28b expression vector (Invitrogen), previously cut with the same enzymes, using T4 DNA ligase (New England Biolabs).

Substitution of Phe-438 by tryptophan was carried out by site-directed mutagenesis using the QuickChange II Site-Directed Mutagenesis kit (Stratagene) and the *Escherichia coli* JM109 strain (Promega), giving rise to plasmid pC-Stk1F438W.

Overexpression and purification of His-tagged C-StkP. Freshly transformed *E. coli* BL21(DE3) cells (Novagen) with the pC-Stk1 or pC-Stk1F438W plasmids were grown in 1 liter of Luria-Bertani (LB) medium [18], supplemented with kanamycin (50 μg/ml) at 37 °C, until OD_{600} = 0.6 was reached. Protein expression was then induced by the addition of 2 mM IPTG, and the culture was allowed to grow for 3 h prior to harvesting of cells. Cells were resuspended in lysis buffer (50 mM sodium phosphate, 300 mM NaCl, 10 mM imidazole, pH 8.0), passed through French pressure (Aminco) and centrifuged at 10 000 *g* for 10 min in order to remove cell debris. The supernatant was then applied onto a Ni-NTA column (Qiagen) (4 ml) and washed extensively with wash buffer (50 mM sodium phosphate, 300 mM NaCl, 10 mM imidazole, pH 8.0). The desired protein was finally eluted from the column with elution buffer (50 mM sodium phosphate, 300 mM NaCl, 250 mM imidazole, pH 8.0), dialyzed against 10 mM ammonium bicarbonate and lyophilized. Protein purity (> 95%) was checked by SDS-PAGE [19] and its concentration was assessed by UV absorption using calculated extinction coefficients [20] of ε_{280} = 7180 M^{-1} cm^{-1} (wild type) and 12750 M^{-1} cm^{-1} (F483W mutant).

Circular dichroism. Circular dichroism (CD) experiments were carried out on a Jasco J-815 spectropolarimeter (Tokyo, Japan) equipped with a Peltier PTC-423S system. Isothermal wavelength spectra were acquired at a scan speed of 50 nm min^{-1} with a response time of 2 s and averaged over at least 4 scans at 25 ºC. Protein concentration was 5.6 μM and the cuvette path-length was 1 mm. Buffer was 20 mM sodium phosphate, 50 mM NaCl, pH 7.0. Ellipticities ([θ]) are expressed in units of (deg cm^2 $dmol^{-1}$), using the residue concentration of protein. Quantification of protein secondary structure was accomplished with the CDNN utilities [21].

For isothermal guanidinium chloride (GdmCl) titrations, aliquots from an 8.0 M denaturant stock solution were added stepwise and incubated for 2 min prior to recording the wavelength spectra. Experiments were repeated at least three times. Equilibrium chemical unfolding data were fitted by least squares to the corresponding two-state process according to equation 1 [22]:

$$\Delta G = \Delta G^{0} - m[\text{GdmCl}] \qquad (1)$$

where ΔG and ΔG^0 are the free energies of unfolding in the presence and absence of GdmCl, respectively, and m represents the dependence of ΔG with respect to the concentration of denaturant. The value of ΔG is calculated using the following equation:

$$\Delta G = -RT \ln K_{eq} = -RT \ln \frac{[\theta]_I - [\theta]_X}{[\theta]_X - [\theta]_F} \qquad (2)$$

where K_{eq} is the equilibrium constant between the initial and final states, $[\theta]_I$ and $[\theta]_F$ are the ellipticities of the initial and final state, respectively, and $[\theta]_X$ is the experimental ellipticity at a given GdmCl concentration. From eqs. (1) and (2) it follows that:

$$\Delta G^{0} = m[\text{GdmCl}]_{½} \qquad (3)$$

where $[\text{GdmCl}]_{½}$ is the midpoint of the denaturation transition.

CD-monitored thermal denaturation experiments were performed in a 1 mm path cell. The sample was layered with mineral oil to avoid evaporation, and the sample was subjected to temperature increases in 10 ºC steps followed by a 5-minute equilibration period and the recording of the corresponding wavelength spectrum.

Fluorescence spectroscopy. Intrinsic fluorescence measurements were carried out at 25 ºC on a PTI-QuantaMaster fluorimeter (Birmingham, NJ, USA), model QM-62003SE, using a 1 × 1 cm path-length cuvette and a protein concentration of 5.6 μM in 20 mM sodium phosphate, 50 mM NaCl, pH 7.0. Tryptophan emission spectra were obtained using an excitation wavelength of 290 nm, with excitation and emission slits of 1 nm and a scan rate of 60 nm min^{-1}. For each experiment, blanks containing buffer and synthetic ligands were subtracted from the recorded spectrum. Experiments were repeated at least three times.

Peptidoglycan isolation. Isolation of crude peptidoglycan (PGN) was essentially performed as described previously [11]. Briefly, cells of *S. pneumoniae* strain Rx1 were cultured in 1 liter of CAT medium) at 37 °C without aeration [23]. Upon reaching an OD_{400} of 1.0, cells were rapidly chilled, harvested and washed using cold 0.8% NaCl solution. Cells were resuspended in 0.8% NaCl solution and added dropwise, under vigorous stirring, into boiling 8% SDS solution. After 1 h the solution was cooled to room temperature, incubated overnight, and the SDS-insoluble cell wall material was subsequently collected by centrifugation. The pellet, containing the cell wall peptidoglycan, was washed several times with water, resuspended in 1.0 ml water and subjected to digestion with mutanolysin (1000 units) overnight at 37 °C. Upon incubation, the protease was inactivated at 80 °C for 20 min. The PGN from *Staphylococcus aureus* was purchased from Sigma-Aldrich.

Peptidoglycan-binding experiments. Approximately 1 mg of PGN was incubated with 25 μg of C-StkP protein in 200 μl of binding buffer (20 mM sodium phosphate, 50 mM NaCl, pH 7.0) for 1 h at 4 °C. Samples were centrifuged (10 min, 20 000 *g*) to remove the soluble fraction. The pellet was then washed once with 200 μl of binding buffer at room temperature for 1 h. PGN-bound proteins were eluted upon resuspension of the pellet in 2% SDS and incubation at room temperature for 1 h, followed by centrifugation. Aliquots from all steps were analyzed by SDS-PAGE. The gels were stained with Coomassie blue. Experiments were performed in triplicate.

RESULTS AND DISCUSSION

The DNA fragment coding for the extracellular C-terminal domain of StkP was cloned into a pET expression vector, giving rise to plasmid pC-Stk1. The expression of the gene produced a protein spanning amino acids 363 to 659 of the full-length StkP plus 20 extra N-terminal residues (arising from the cloning procedures and containing the hexahistidine tag and 4 residues belonging to the N-terminal moiety of the protein), and which is referred to hereafter as C-StkP (Fig. 2). The protein was purified to an extent higher than 95% according to SDS-PAGE analysis (data not shown). Most of the amino acids have been predicted to constitute four PASTA motifs (p1 to p4) [14], among which p2 and p3 are the most similar to each other (Fig. 2). A PSI-BLAST search carried out by the PHYRE server identified the PASTA sequences comprising residues 633-750 of the pneumococcal penicillin-binding protein PBP2x (PDB code 1QMF) as a suitable template for the modeling of C-StkP, the PASTA sequences of which display an average of 15% identity and 29.5% similarity. These moderate values are usually encountered in otherwise structurally similar PASTA domains [8], an observation that suggests that the PASTA architecture is able to accommodate a high sequence variability. The first of the PBP2x PASTA motifs showed the highest similarity with the StkP domains (Supplementary Fig. S1) and was therefore used as a template for modeling studies. This was accomplished with the SwissPDB utilities (see Materials and Methods), and the resulting structure suggests that each PASTA motif consists of an α-helix packed onto a three-stranded antiparallel β-sheet (Fig. 3), as described earlier for a related system [9]. We note that there exists some uncertainty on the structures of the loops linking the PASTA sequences, due to the lack of similarity with the template in these regions. It might be argued that the recently elucidated structure of the PASTA domain of the *Mycobacterium tuberculosis* PknB kinase [8] might constitute a better template since it already contains four consecutive PASTA domains, similarly

to C-StkP, and also displays a good sequence similarity (Supplementary Figure S1). However, the extended structure of the former is not compatible with our thermodynamic results, as described below.

In order to validate our three-dimensional model, we obtained the far-UV circular dichroism (CD) spectrum of C-StkP (Fig. 4A). The spectrum displays a broad negative band, whose mathematical deconvolution revealed a secondary structure content of 15% α-helix, 30% β-sheet and 55% other structures, consistent with that predicted by the model (14% α-helix, 25% β-sheet and 61% other structures) within the limits of CD deconvolution methods (Fig. 3). Furthermore, we checked the thermodynamic stability of the protein at neutral pH and 20 ºC by means of equilibrium denaturation experiments with guanidinium chloride (GdmCl), monitored by CD (Fig. 4B). The existence of a cooperative transition confirmed that the purified protein was properly folded. Interestingly, only one denaturation transition was detected, despite the existence of four PASTA motifs, suggesting that these sequences interact strongly among themselves, hence the protein denatures as a single cooperative unit. This hypothesis receives additional support from the thermal denaturation experiment shown in Fig. 4C, which also displays a single unfolding transition. These results are more in concordance with the configuration of PASTA sequences in PBP2x than that in PknB, where the extended arrangement of motifs would likely originate partly folded intermediates arising from the independent unfolding of domains, in turn giving rise to multiple, sequential transitions. Moreover, such cooperativity is to be expected for a domain that transduces the signal to the intracellular domain via conformational changes. All changes induced by GdmCl turned out to be reversible upon denaturant elimination (data not shown). Thermodynamic analysis of the denaturation curve in Fig. 4B using Eqs. 1-3 allowed us to calculate the corresponding unfolding parameters: $m = 7.1 \pm 0.4$ kJ mol^{-1} M^{-1}, $[\text{GdmCl}]_{½} = 2.2 \pm 0.1$ M, and a free energy of unfolding $\Delta G^{o} = 16.3 \pm 0.4$ kJ mol^{-1}, that lies within the typical range for a globular protein [24].

Crystallographic analysis of cefuroxime-bound PBP2x from *S. pneumoniae* has pointed to PASTA sequences as binding motifs for β-lactam antibiotics [9]. We decided to investigate whether C-StkP was also capable of interacting with these antibiotics, such as ampicillin (**1**, Fig. 1). To do so, we recorded the CD spectrum of a solution containing C-StkP and ampicillin (**1**), and compared the result with the theoretical sum of the corresponding spectra obtained separately. As shown in Fig. 5 (upper panel), we found a small but highly reproducible difference between the experimental and theoretical CD data, that accounts for approximately 10% of the signal in the 235-240 nm region (Fig. 5, upper panel, inset). These variations cannot be ascribed to mere differences in concentration of the compounds since the ellipticities around 210 nm, with higher absolute intensity than those at 240 nm, are however virtually coincident. On the other hand, the CD change is localized in a wavelength region that does not correspond to amide bond absorption bands [25], so it might rather reflect a change in conformation of bound ampicillin. This also suggests that the secondary structure of the protein does not change at a significant level upon antibiotic binding.

In any case, the small variations observed in the CD spectra, due to the high background signal of the ligands prompted us to carry out an alternative study with other molecules that originate less interference problems. Since, according to Tipper and Strominger [10], β-lactam molecules emulate the structure of the D-Ala-D-Ala sequence in the peptidic linkers of the peptidoglycan, we analyzed the binding of this dipeptide to C-StkP by fluorescence spectroscopy. As depicted in Fig. 5 (middle panel), the D-Ala-D-Ala dipeptide binds to the protein and induces an increase in the fluorescence intensity in a similar vein than bigger peptidoglycan units (see below). This result supports our hypothesis on the effective interaction of ampicillin and 6-APA with C-StkP.

As stated above, it has been previously described that binding of cefuroxime to PBP2x occurs through interactions of the β-lactam ring with the PASTA sequence. Therefore, in order to map the part

of the ampicillin molecule that interacts with C-StkP, we performed CD-monitored binding experiments with 6-aminopenicillanic acid (6-APA, **2**). Results depicted in Fig. 5 (lower panel and inset) confirm the interaction of the β-lactam moiety with the protein. In this case the conformational change of the ligand leads to a CD difference spectrum of opposite sign to that of ampicillin (**1**, Fig. 5A, inset), probably due to the lack of contribution to the spectrum of the phenyl group in the former molecule. This result strongly suggests that the PASTA motifs in C-StkP constitute binding sites for β-lactam antibiotics in general.

The structure of the penicillin backbone extending from the C_3 carboxylate to the substituent at the C_6 mimics the non-crosslinked terminal portion of the peptide stem of the peptidoglycan according to the thesis of Tipper and Strominger [10]. PASTA-containing proteins such as pneumococcal PBP2x, the *Mycobacterium tuberculosis* PknB kinase and related homologues, or the PrkC serine/threonine kinase from *Bacillus subtilis* have been suggested to interact with peptidoglycan (PGN) fragments to trigger their signaling functions [6,8] and the backbone of β-lactam antibiotics is believed to exploit this recognition based on the mimicry. To explore whether PASTA repeats are determinants of peptidoglycan binding for the pneumococcal StkP kinase, we first determined whether the C-StkP domain could bind to crude PGN preparations. As shown in Fig. 6A, incubation of 25 μg C-StkP with 1 mg of purified pneumococcal PGN and subsequent centrifugation of the sample localized about 40% of the protein in the insoluble (PGN) fraction. In order to detect any non-specific interactions between the two, C-StkP was also incubated in parallel with PGN from *S. aureus* in the same conditions, but in this case virtually none of the protein was found associated with the peptidoglycan (Fig. 6B). This result strongly suggests that C-StkP recognizes specifically the pneumococcal PGN. Although *S. aureus* and *S. pneumoniae* peptidoglycans share the same stem peptide sequence, the degree of crosslinking is distinct [26,27]. This creates differences in the structure of the cell wall in the two organisms, leading

to a different accessibility of C-StkP to the binding sites, likely due to steric reasons. In support of this idea, a species-specific binding of PGN by PASTA-containing protein kinases has already been described in some cases [11].

Having provided evidence that crude samples of PGN from *S. pneumoniae* can bind to C-StkP, we explored whether a synthetic sample of PGN would do the same. The synthetic samples represent a single repeat unit of the building unit of the peptidoglycan, namely *N*-acetylglucosamine (NAG)-*N*-acetylmuramyl (NAM) (compound **3**) with the associated pentapeptide and a more minimalist molecule lacking the NAG unit (compound **4**) (Fig. 1). In this case, we did not observe a significant change in the far-UV CD spectra even using 2.5 mM ligand (data not shown). This would suggest either that there is no binding or that the structures of neither the protein nor the ligand changed to a significant level upon binding. In order to discriminate between these two possibilities, we substituted Phe-438 in C-StkP by tryptophan (C-StkP[F438W] protein) by site-directed mutagenesis with the aim of monitoring subtle conformational changes induced by the ligands with the more sensitive fluorescence spectroscopy. Phe-438, in the N-terminal part of the PASTA motif p2 (Fig. 2) was chosen since, according to our structural model, a Trp residue in this position could be readily accommodated without seriously disturbing the overall packing of the protein and would not interfere with the presumed ligand-binding site [9] (data not shown). As shown in Fig. 7A, addition of either compound **3** or **4** in millimolar concentrations caused an increase in the fluorescence intensity of the protein. The change was more evident in the case of **3**, demonstrating the importance of the NAG moiety in binding (Fig. 1). The specificity of **3** binding to C-StkP can be ascertained from the titration curve shown in Fig. 7B, that displays saturation at the highest ligand concentration assayed. Furthermore, high concentrations of compound **3** did not affect the fluorescence spectrum of an unrelated protein such as the response regulator StyR from *Pseudomonas* sp. Y2 [28] (Fig. 7B), which serves as a negative control. To our knowledge, this is the first direct documentation of recognition of a minimal PGN unit

by a PASTA-containing protein kinase. It is important to note that the affinity of C-StkP for either the synthetic PGN samples or β-lactam antibiotics is rather low, in the millimolar range, which is consistent with the hypothesis that PASTA domains guide the localization of the entire protein in the PGN through loose interactions [3]. We hasten to add that the cases of binding of proteins to multivalent ligands, such as the polymeric PGN, might be different. The improved contribution to binding from polymeric PGN could originate from a favourable entropic factor. This assertion is supported by the positive outcome of the pull-down experiment with the PGN preparations shown in Fig. 6A, indicating that favourable multivalent interactions of C-StkP within the macromolecular peptidoglycan structure are likely to exist.

CONCLUDING REMARKS

We present here the first biophysical evidence of the specific interaction of the pneumococcal eukaryotic-type serine/threonine protein kinase StkP with synthetic peptidoglycan samples and with β-lactam antibiotics. This confirms the previous suggestions that PASTA motifs in several proteins function as sensors of non-crosslinked peptidoglycan to trigger signal transduction. This hypothesis has recently received experimental support by Shah *et al* [11], who found that the PrkC protein from *B. subtilis* binds to preparations of peptidoglycan from bacteria. Our results are further consistent with this assertion and provide evidence that synthetic peptidoglycan samples such as **3** and **4** as minimal structures are capable of binding to StkP kinase. Given the high panoply of cellular functions in which StkP is involved [13], it will be of great interest to investigate how these are affected upon contact of the kinase to peptidoglycan fragments. Finally, our data also demonstrate the recognition of β-lactam antibiotics by StkP and support the notion of the PASTA-containing proteins as interesting targets for these antibiotics, which should be considered in the future for the design of new antimicrobials against *S. pneumoniae*.

ACKNOWLEDGMENTS

This work was supported by grants BIO2007-67304-C02-02 and BFU2010–17824 (Spanish Ministry of Education), EU-CP223111 (CAREPNEUMO, European Union), 204/07/P082 and 204/08/0783 (both by Czech Science Foundation), IAA600200801 by The Grant Agency of the Academy of Sciences of the Czech Republic, Institutional Research Concept no. AV0Z50200510 and by a grant from the National Institutes of Health for the research in the USA. We thank M. Gutiérrez for excellent technical assistance. E.L. was a recipient of a Beca de Colaboración from the Spanish Ministry of Education.

REFERENCES

[1] Hoch, J.A. (2000). Two-component and phosphorelay signal transduction. *Curr. Opin. Microbiol*. 3, 165-170.

[2] Stock, A.M., Robinson, V.L., and Goudreau, P.N. (2000). Two-component signal transduction. *Annu. Rev. Biochem.* 69, 183-215.

[3] Jones, G., and Dyson, P. (2006). Evolution of transmembrane protein kinases implicated in coordinating remodeling of Gram-positive peptidoglycan: inside versus outside. *J. Bacteriol.* 188, 7470-7476.

[4] Krupa, A., and Srinivasan, N. (2005). Diversity in domain architectures of Ser/Thr kinases and their homologues in prokaryotes. *BMC Genomics* 6, 129.

[5] Av-Gay, Y., Jamil, S., and Drews, S.J. (1999). Expression and characterization of the *Mycobacterium tuberculosis* serine/threonine protein kinase PknB. *Infect. Immun*. 67, 5676-5682.

[6] Yeats, C., Finn, R.D., and Bateman, A. (2002). The PASTA domain: a β-lactam-binding domain. *Trends Biochem. Sci*. 27, 438-440.

[7] Pares, S., Mouz, N., Pétillot, Y., Hakenbeck, R., and Dideberg, O. (1996). X-ray structure of *Streptococcus pneumoniae* PBP2x, a primary penicillin target enzyme. *Nat. Struct. Biol*. 3, 284-289.

[8] Barthe, P., Mukamolova, G.V., Roumestand, R. and Cohen-Gonsaud, M. (2010). The structure of PknB extracellular PASTA domain from *Mycobacterium tuberculosis* suggests a ligand-dependent kinase activation. *Structure* 18, 606–615.

[9] Gordon, E., Mouz, N., Duée, E. and Dideberg, O. (2000). The crystal structure of the penicillin-binding protein 2x from *Streptococcus pneumoniae* and its acyl-enzyme form: implication in drug resistance. *J. Mol. Biol*. 299, 477-485.

[10] Tipper, D.J. and Strominger, J.L. (1965). Mechanism of action of penicillins: a proposal based on their structural similarity to acyl-D-alanyl-D-alanine. *Proc. Natl. Acad. Sci. USA*. 54, 1133-1141.

[11] Shah, I. M., Laaberki, M-H., Popham D.L., and Dworkin, J. (2008). A eukaryotic-like Ser/Thr kinase signals bacteria to exit dormancy in response to peptidoglycan fragments. *Cell* 135, 486-496.

[12] Pallová, P., Hercík, K., Sasková, L., Nováková, L., and Branny, P. (2007). A eukaryotic-type serine/threonine protein kinase StkP of *Streptococcus pneumoniae* acts as a dimer *in vivo*. *Biochem. Biophys. Res. Commun.* 355, 526-530.

[13] Sasková, L., Nováková, L., Basler, M., and Branny, P. (2007). Eukaryotic-type serine/threonine protein kinase StkP is a global regulator of gene expression in *Streptococcus pneumoniae. J. Bacteriol.* 189, 4168-4179.

[14] Nováková, L., Sasková, L., Pallová, P., Janeček, J., Novotná, J., Ulrych, A., Echenique, J., Trombe, M-C., and Branny, P. (2005). Characterization of a eukaryotic type serine/threonine protein kinase and protein phosphatase of *Streptococcus pneumoniae* and identification of kinase substrates. *FEBS J.* 272, 1243-1254.

[15] Hesek, D., Lee, M., Morio, K.-I., and Mobashery, S. (2004). Synthesis of a fragment of bacterial cell wall. *J. Org. Chem*. 69, 2137-2146.

[16] Hesek, D., Suvorov, M., Morio, K.-I., Lee, M., Brown, S., Vakulenko, S.B., and S. Mobashery. (2004). Synthetic peptidoglycan substrates for penicillin-binding protein 5 (PBP5) of Gram-negative bacteria. *J. Org. Chem*. 69, 778-784.

[17] Guex, N., and Peitsch., M.C. (1997). SWISS-MODEL and the Swiss-PdbViewer: an environment for comparative protein modeling. *Electrophoresis* 18, 2714-2723.

[18] Sambrook, J., Fritsch, E.F., and Maniatis, T. (1989). Molecular cloning: a laboratory manual, 2nd ed. Cold Spring Harbor Laboratory Press, Cold Spring Harbor, N.Y.

[19] Laemmli, U.K. (1970). Cleavage of structural proteins during the assembly of the head of bacteriophage T4. *Nature* 227, 680–685.

[20] Fasman, G.D. (ed.). 1976. Handbook of biochemistry and molecular biology. Section A: Proteins, 3rd ed., vol. III. CRC Press, Inc., Cleveland, Ohio.

[21] Bohm, G., Muhr., R. and Jaenicke, R. (1992). Quantitative analysis of protein far UV circular dichroism spectra by neural networks. *Protein Eng*. 5, 191–195.

[22] Greene, R. F. Jr., and Pace., C.N. (1974). Urea and guanidinium chloride denaturation of ribonuclease, lysozyme, α-chymotrypsin, and β-lactoglobulin. *J. Biol Chem*. 249, 5388-5393.

[23] Morrison, D.A., Lacks, S.A., Guild, W.R., and Hageman, J.M. (1983). Isolation and characterization of three new classes of transformation-deficient mutants of *Streptococcus pneumoniae* that are defective in DNA transport and genetic recombination. *J. Bacteriol.* 156, 281-290.

[24] Creighton, T.E. (1993). Proteins: structures and molecular properties, 2nd ed, W.H. Freeman and co., U.S.A.

[25] Johnson, W.C. (1990). Protein secondary structure and circular dichroism: a practical guide. *Proteins Struct. Funct. Genet*. 7, 205-214.

[26] García-Bustos, J.F., Chait, B.T. and Tomasz. A. (1987). Structure of the peptide network of pneumococcal peptidoglycan. *J. Biol. Chem*. 262, 15400-15405.

[27] Navarre, W.W., Ton-That, H., Faull, K.F., and Schneewind, O. (1999). Multiple enzymatic activities of the murein hydrolase from staphylococcal phage ϕ11. Identification of a D-alanyl-glycine endopeptidase activity. *J. Biol. Chem*. 274, 15847–15856.

[28] Velasco, A., Alonso, S., García, J.L., Perera J., and Díaz, E. (1998). Genetic and functional analysis of the styrene catabolic cluster of *Pseudomonas* sp. strain Y2. *J. Bacteriol*. 180, 1063-1071.

LEGENDS TO FIGURES

Figure 1. Chemical structures of ampicillin (**1**), 6-aminopenicillanic acid (**2**) and synthetic peptidoglycan fragments **3** and **4**.

Figure 2. Amino acid sequence of recombinant C-StkP. Sequence-aligned predicted PASTA motifs, represented by p1 to p4, are shown aligned upon using the CLUSTALW utilities in the NPSA server (http://npsa-pbil.ibcp.fr/cgi-bin/npsa_automat.pl?page=/NPSA/npsa_server.html). Identities are shown in bold and indicated by asterisk (*), whereas highly conservative changes are identified by a colon (:) and less conservative changes are indicated by a dot (.). Phe-438 is highlighted in bold underlined italic.

Figure 3. Left: The three-dimensional homology model of the C-StkP structure, displaying the p1-p4 motifs and the Phe-438 residue (in spacefill representation). Right: Secondary structure assignments to the C-StkP primary structure. α-helices are represented as red cylinders, β-structures are shown as yellow arrows, and other structures (loops and irregular conformations) are displayed as dashed rectangles.

Figure 4. (A) Far-UV CD spectrum of C-StkP. (B) Monitoring of equilibrium unfolding of C-StkP by CD. (C) Thermal unfolding of C-StkP monitored by following the CD signal at 205 nm. A sigmoidal curve is shown only for presentation purposes and has no thermodynamic meaning.

Figure 5. *Upper panel*, interaction of 5.6 μM C-StkP with 1 mM ampicillin (**1**) monitored by CD at 25 ºC in 20 mM sodium phosphate, 50 mM NaCl, pH 7.0; the solid line is the experimental spectrum of the complex, and the dashed line is the theoretical spectrum obtained by the sum of the spectra of protein and ligand recorded separately. The *inset* shows the difference in ellipticity between experimental and theoretical spectra. Experiments were repeated four independent times and a typical result is shown in the figure; *middle panel*, intrinsic fluorescence spectrum of 5.6 μM C-StkP (solid line) and 5.6 μM C-StkP plus 1 mM D-Ala-D-Ala (dashed line); *lower panel*, interaction of 5.6 μM C-StkP with 1 mM 6-APA (**2**) monitored by CD. Conditions and line patterns as in the upper panel.

Figure 6. (A) Interaction of C-StkP with crude peptidoglycan preparations from *S. pneumoniae*. Lane 1, soluble fraction after binding and centrifugation; lane 2, wash fraction; lane 3, total protein release from incubation of PGN with SDS. (B) Interaction of C-StkP with crude peptidoglycan preparations from *S. aureus*. Lane 1, soluble fraction after binding and centrifugation; lane 2, wash fraction; lane 3, total protein release from incubation of PGN with SDS.

Figure 7. (A) Interaction of 5.6 μM C-StkP[F438W] with 2.5 mM compound **3** or 2.5 mM compound **4** monitored by tryptophan fluorescence spectroscopy. Solid line, protein only; dashed line, protein + **4**; dotted line, protein + **3**. (B) Fluorescence-monitored titration of C-StkP[F438W] with **3**, followed by fluorescence emission at 340 nm (excitation at 290 nm) (closed circles); effect of compound **3** on the fluorescence of the unrelated protein StyR (open circles marked by arrows). StyR concentration was chosen to be 4.8 μM, so that the fluorescence intensity in the absence of ligand matched that of C-StkP[F438W], to facilitate comparison.

LEGENDS TO SUPPLEMENTARY FIGURES

Supplementary Figure S1. (A) CLUSTALW alignment analysis of individual PASTA motifs of StkP with the first PASTA sequence of pneumococcal PBP2x. (B) Alignment of the PASTA motifs from StkP and PknB. Identities are shown in bold and indicated by asterisk (*), whereas highly conservative changes are identified by a colon (:) and less conservative changes are indicated by a dot (.).

Figure 1

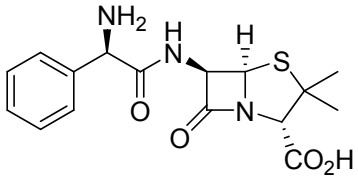

1 (Ampicillin)

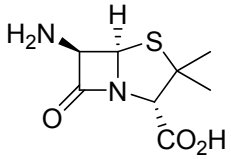

2 (6-APA)

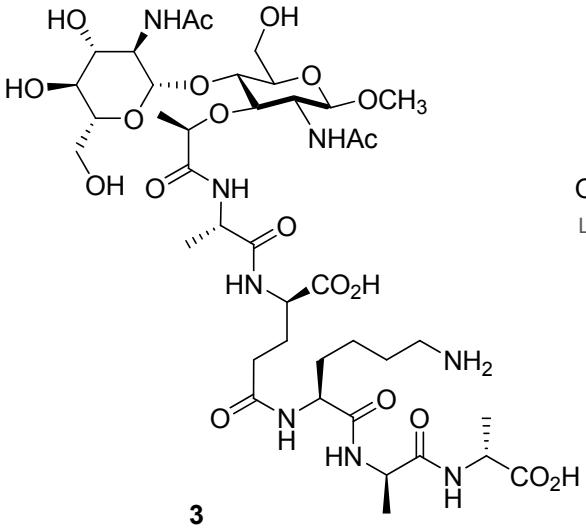

3

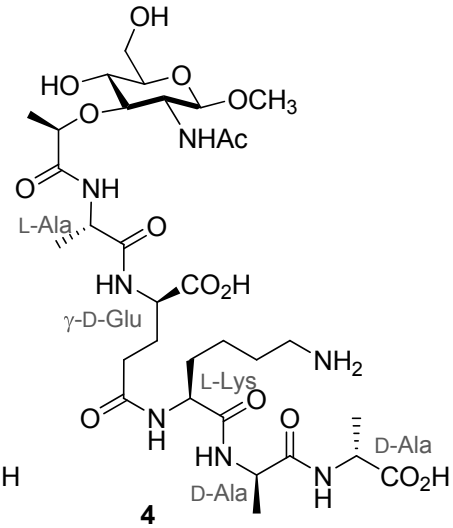

4

Figure 2

Additional residues from cloning (-20 to -1): MGSSHHHHHHSSGLVPRGSH

N-terminal residues belonging to StkP (363 to 366): MSRS

```
p1  (367 to 433):      -PATIAIPDVAGQ----TVAEAKATLKKANF--EIGEEKTEASEKVEEGRIIRTDPGAGT--GRKEGTKINLVVSS
p2  (434 to 505):      GKQSFQISNYVGR----KSSDVIAELKEKKVPDNLIKIEEEESNESEAGTVLKQSLPEGTTYDLSKATQIVLTVAK
p3  (506 to 577):      KATTIQLGNYIGR----NSTEVISELKQKKVPENLIKIEEEESSESEPGTIMKQSPGAGTTYDVSKPTQIVLTVAK
p4  (578 to 651):      KVTSVAMPSYIGSSLEFTKNNLIQIVGIKEANIEVVEVTTAPAGSVE-GMVVEQSPRAGEKVDLNK-TRVKISIYK
                          :. : .  *     .  :    :   :   :: :     : . * * ::. .   *   . .: *:: : : .
```

C-terminal tail (652 to 659): PKTTSATP

Figure 3

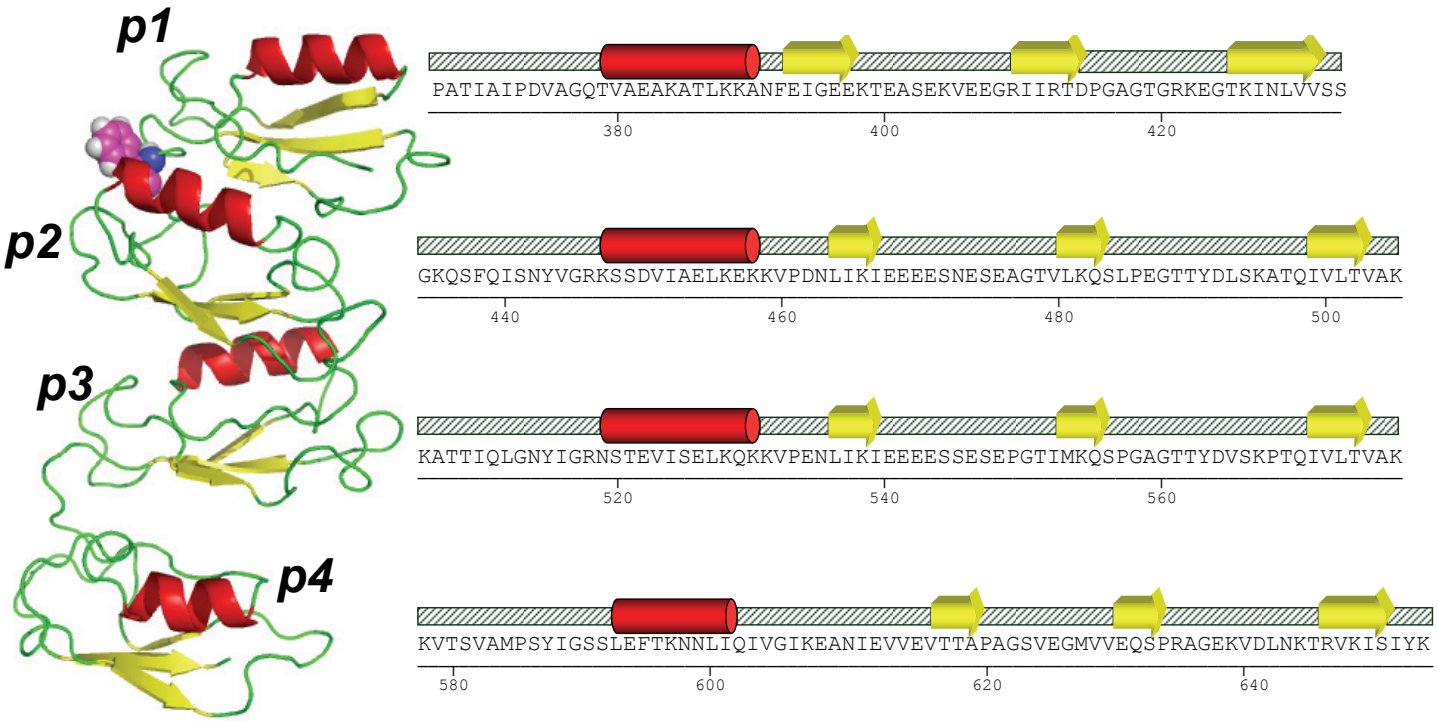
p1
p2
p3
p4
PATIAIPDVAGQTVAEAKATLKKANFEIGEEKTEASEKVEEGRIIRTDPGAGTGRKEGTKINLVVSS
380
400
420
GKQSFQISNYVGRKSSDVIAELKEKKVPDNLIKIEEEESNESEAGTVLKQSLPEGTTYDLSKATQIVLTVAK
440
460
480
500
KATTIQLGNYIGRNSTEVISELKQKKVPENLIKIEEEESSESEPGTIMKQSPGAGTTYDVSKPTQIVLTVAK
520
540
560
KVTSVAMPSYIGSSLEFTKNNLIQIVGIKEANIEVVEVTTAPAGSVEGMVVEQSPRAGEKVDLNKTRVKISIYK
580
600
620
640

Figure 4

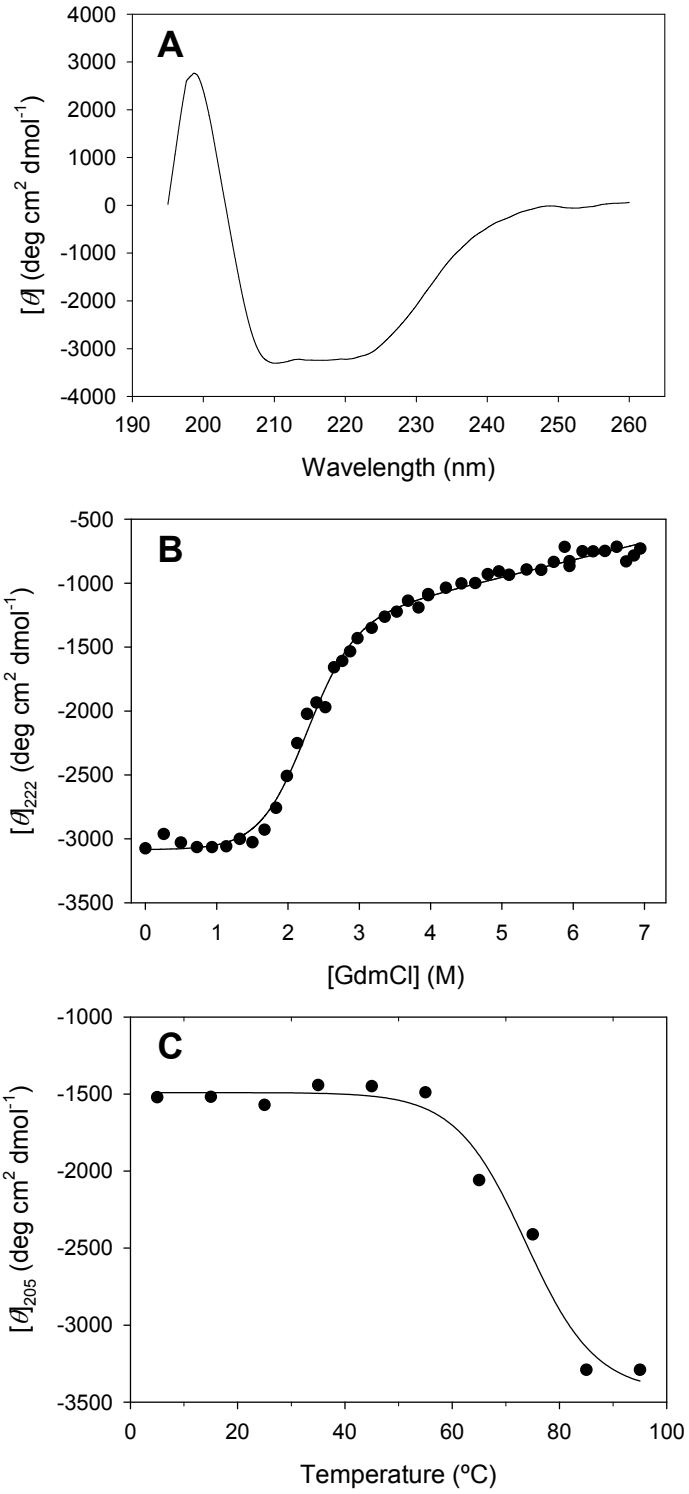
A
4000
3000
2000
1000
0
-1000
-2000
-3000
-4000
190
200
210
220
230
240
250
260
Wavelength (nm)
[ϑ] (deg cm2 dmol-1)
B
-500
-1000
-1500
-2000
-2500
-3000
-3500
0
1
2
3
4
5
6
7
[GdmCl] (M)
[ϑ222 (deg cm2 dmol-1)
C
-1000
-1500
-2000
-2500
-3000
-3500
0
20
40
60
80
100
Temperature (ºC)
[ϑ205 (deg cm2 dmol-1)

Figure 5

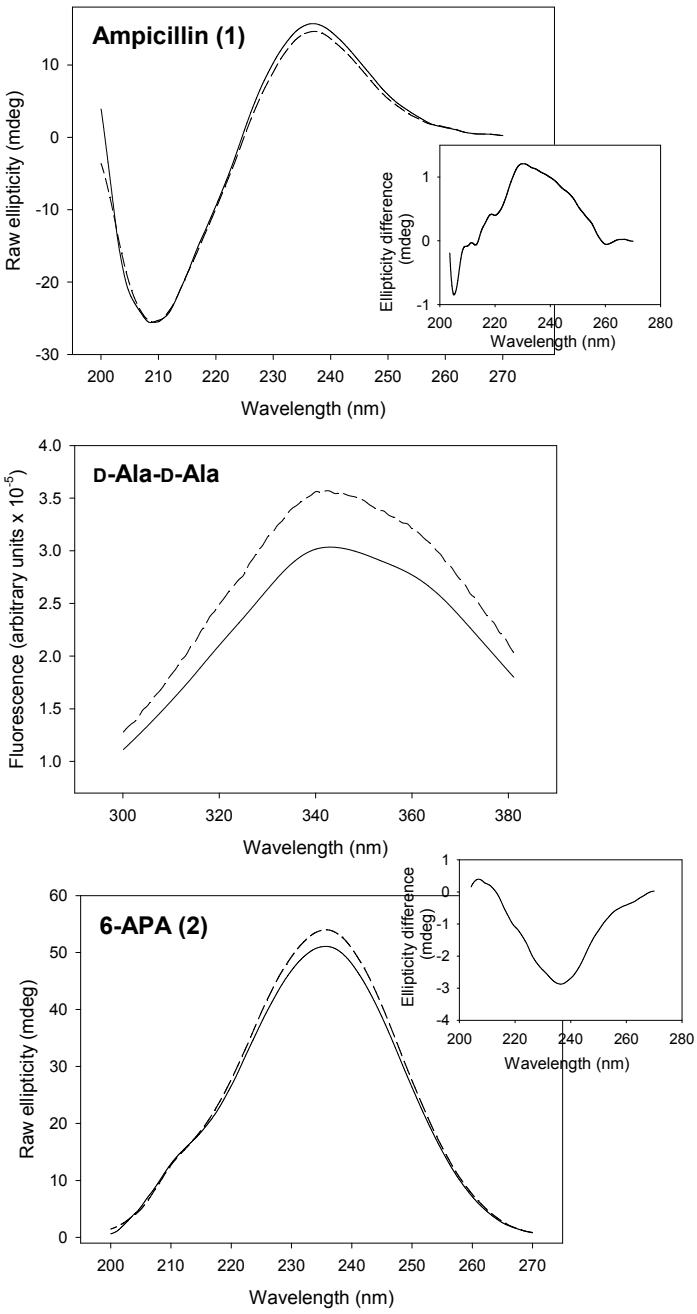
Ampicillin (1)
Raw ellipticity (mdeg)
Wavelength (nm)
Ellipticity difference (mdeg)
Wavelength (nm)
D-Ala-D-Ala
Fluorescence (arbitrary units x 10-5)
Wavelength (nm)
6-APA (2)
Raw ellipticity (mdeg)
Wavelength (nm)
Ellipticity difference (mdeg)
Wavelength (nm)

Figure 6

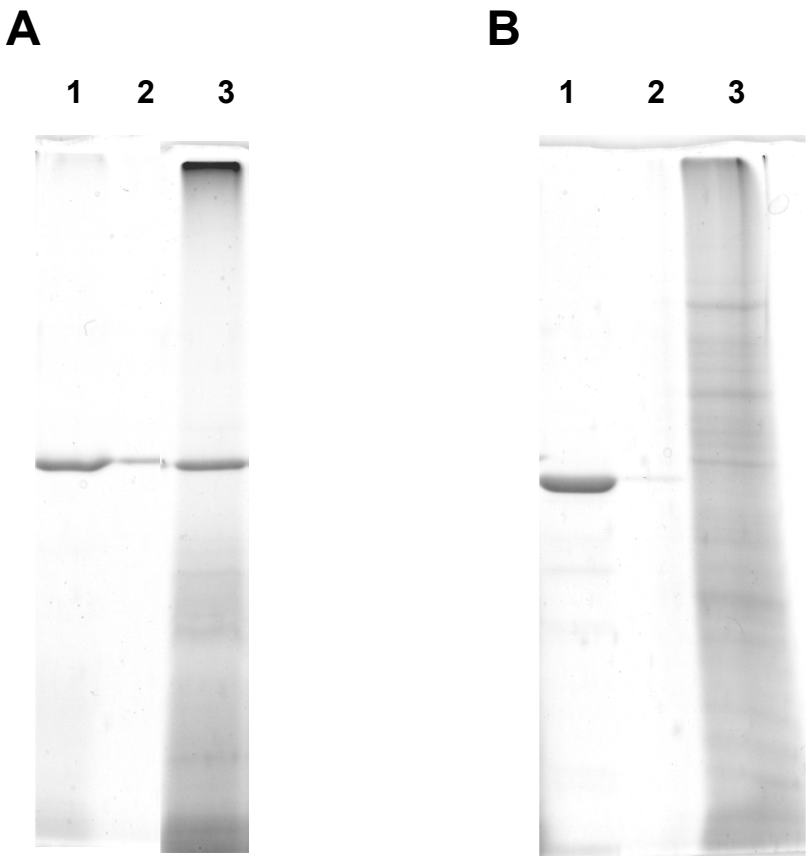

Figure 7

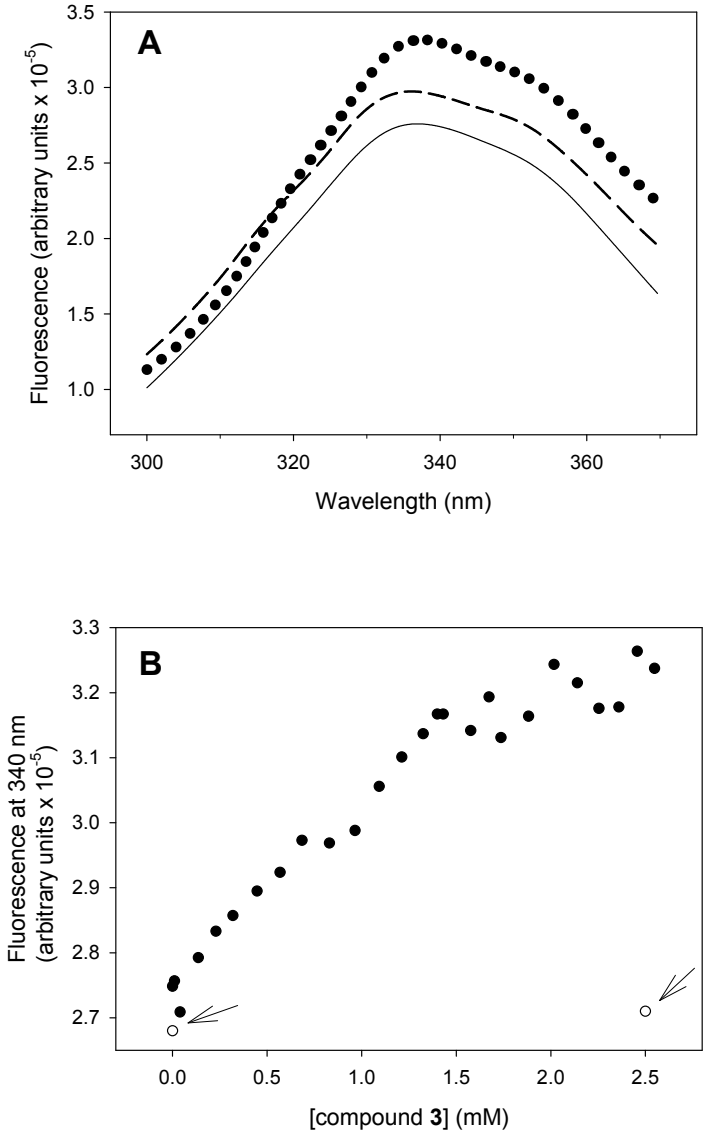
A
Fluorescence (arbitrary units x 10-5)
3.5
3.0
2.5
2.0
1.5
1.0
300
320
340
360
Wavelength (nm)
B
Fluorescence at 340 nm
(arbitrary units x 10-5)
3.3
3.2
3.1
3.0
2.9
2.8
2.7
0.0
0.5
1.0
1.5
2.0
2.5
[compound 3] (mM)